Statics and Dynamics of the Benard Convection Rolls in an Intermediate-Aspect-Ratio Vessel

AUTHOR(S):

YAHATA, Hideo

CITATION:

YAHATA, Hideo. Statics and Dynamics of the Benard Convection Rolls in an Intermediate-Aspect-Ratio Vessel. 数理解析研究所講究録 1989, 677: 118-133

ISSUE DATE:

1989-01

URL:

http://hdl.handle.net/2433/101021

数理解析研究所講究録118
第677巻 1989年 118-133

Statics and Dynamics of the Benard Convection Rolls in an Intermediate-Aspect-Ratio Vessel[1]

Hideo YAHATA
Department of Materials Science, Faculty of Science
Hiroshima University, Hiroshima 730

Spatial structure and temporal evolution of thermal convection appearing in an intermediate-aspect-ratio box are studied using a model system of coupled-mode equations. The model simultaneously contains two kinds of the mode variables each representing the convection roll state with a definite total number of the rolls. The two are different from each other in the associated total number of the rolls. The 112-mode system is used to clarify spatial and temporal behavior of the convection rolls appearing in a rectangular box of proportions $10\times4\times1$ at the Prandtl number $\sigma=7$. Actual computations were performed for several chosen sets of the total number of the rolls. For the model consisting of the 6- and 10-roll states, the transition from the 10- to the 6-roll state occurs with an increase of the Rayleigh number R, and an oscillatory motion with the frequency of the order of 10 mHz appears at higher Rayleigh numbers. By contrast, for the model consisting of the 6- and the 8-roll states, the 6-roll state dominates the spatial pattern over a wide range of R , and the system at higher values of R develops extremely slow oscillations with the frequency of the order of 1 mHz. Finally, for the model consisting of the 6- and the 12-roll states, although the 6-roll state likewise dominates the spatial pattern, the frequency of the oscillatory motion at higher values of R turns out to be of the order of 100 mHz, which is comparable to that widely observed in convection experiments on small-aspect-ratio systems.

[1]Unfinished and subject to revision

§1. Introduction

The Rayleigh-Benard convection is one of the typical nonlinear dissipateve systems which involve instabilities leading to a variety of spatio-temporal flow structure. Experiments are usually performed for a fluid confined in a rectangular or a cylindrical vessel. For this type of closed flow systems the aspect ratio of the vessel Γ has a crucial influence in determining the manner in which instabilities occur and the resulting convection patterns develop. For small-aspect-ratio rectangular systems ($\Gamma<5$), convection usually appears in the form of a small number of rolls and its overall spatial pattern remains unchanged over a wide range of the vertical thermal gradient or the Rayleigh number R . For the past ten years, many experimental and theoretical studies have been performed on this type of systems to clarify the mechanism underlying the transition from periodic to chaotic oscillations of convection.[1),2)] The results show that oscillatory convection with increase of R undergoes various types of successive bifurcations leading to chaos and that these experimental facts are well described using model dynamical systems consisting of only a small number of variables. On the other hand, for large aspect-ratio systems ($\Gamma >20$), convection does not reach a steady regular pattern even after lapse of an enormously long time comparable to the lateral thermal diffusion time. As a result, it never ceases to exhibit irregular temporal behavior even only slightly above R_c where R_c denotes the critical Rayleigh number at which thermal conduction state becomes unstable.[3)]

In the face of these experimental results for the small and the large aspect-ratio systems, several research groups recently made experiments on convection appearing in intermediate-aspect-ratio systems ($\Gamma \sim 10$) where the aspect ratio is large enough to allow transitions between different spatial patterns for some higher values of R, but, at the same time, small enough to give rise to stable regular patterns over a wide range of R above R_c.[4)~6)] The experimental results show that convection in several

respects exhibits behavior quite peculiar to the external conditions specified now as *intermediate*. Convection first sets in in the form of the periodic structure consisting of parallel horizontal rolls where their axes are parallel to the shorter sides of the rectangular cell. When R is increased, these rolls undergo a spatial transition leading to the rolls with a larger period. This was particularly clearly shown using a shadow graph method. For example, the experiment using water ($\sigma = 7$) in a rectangular cell specified by $\Gamma_x = 10$ and $\Gamma_y = 4$ reveals that the 10-roll state appearing at $R = R_c$ =1710 from thermal conduction state undergoes at $R = 8.6R_c$ a transition to the 6-roll state.[5] The experimentally observed value of R at which this transition occurs agrees quite well with the theoretical value for the onset of the skewed-varicose (SV) instability obtained by Busse et al. for an infinitely extended roll system.[7] With further increase of R, the convection develops extremely slow oscillatory motion with the frequency of the order of 1 mHz. We here refer to the fact that the frequencies of the oscillatory convection typically observed in small-aspect-ratio systems are usually of the order of 100 mHz. Although the amplitude of this slow oscillations is weak, the associated field is almost uniformly distributed over the whole range of the rectangular cell. At still higher values of R, convection further develops additional periodic motion whose frequencies are of the order of 100 mHz. However, some experimental reports emphasize that these fluid oscillators are situated only over certain localized regions of the cell.[8),9] This partially accouts for the salient experimental results for intermediate-aspect-ratio systems that nonchaotic oscillatory convection under certain conditions contains as many as four or five incommensurate frequencies.

The purpose of the present paper is to study thermal convection in an intermediate-aspect-ratio vessel using a system of Galyorkin equations for the roll mode variables. In previous papers,[10] the author used this type of model equations governing temporal evolution of the roll modes in order to clarify bifurcation routes to chaos in small-

aspect-ratio systems. For the present case, it is necessary to extend the system of model equations by including additional relevant roll variables in such a way that it involves structural transitions between the convection states whose wavelengths of the rolls are different from each other. This extension necessarily influences dynamical behavior of the roll mode variables. Hence, the extended model system thus obtained is expected to describe both spatial and temporal behavior of thermal convection in intermediate-aspect-ratio systems.

§2. Basic equations of motion

In this section derivation of the basic equations of motion is briefly presented. A fluid is contained in a rectangular box heated from below. Let x, y, z denote the rectangular coordinates with the z axis directed upward. The aspect ratios of the box are defined as $\Gamma_x = L_x/d$ and $\Gamma_y = L_y/d$ where L_x, L_y and d denote the side length of the box in the x, y and z direction. The physical quantities used in this paper are denoted as follows: ρ is the density of the fluid, ν is the kinematic viscosity, κ is the thermal diffusivity, α is the thermal expansion coefficient,g is the gravitational constant and T_d is the temperature difference between the two horizontal boundaries. For the non-dimensional description of the equations of motion, the length scale d, the time scale d^2/κ and the temperature scale $\kappa\nu/g\alpha d^3$ are used. Within the framework of the Boussinesq approximations, thermal convection is governed by the disturbance equations of motion for the velocity $\mathbf{u}=(u_x, u_y, u_z)$, the temperature θ and the pressure δp in the form

$$\partial_t u_i - \sigma \Delta u_i - \sigma\delta_{i,z}\theta + \partial_i(\delta p/\rho) = -u_j\partial_j u_i, \quad (i = x, y, z) \tag{1}$$

$$\partial_t\theta - \Delta\theta - Ru_z = -u_j\partial_j\theta, \tag{2}$$

$$\partial_i u_i = 0 \tag{3}$$

where $\sigma = \nu/\kappa$ is the Prandtl number, $R = g\alpha d^3 T_d/\kappa\nu$ is the Rayleigh number and $\delta_{i,j} = 1(i = j); = 0(i \neq j)$. The boundary conditions(b.c.) are assumed to be as follows:

u obeys the rigid b.c.; θ obeys the isothermal and adiabatic b.c. on the horizontal and the lateral walls respectively. When the domain occupied by the fluid is defined by $(-\Gamma_x/2, \Gamma_x/2) \times (-\Gamma_y/2, \Gamma_y/2) \times (-1/2, 1/2)$, these boundary conditions are written in the form

$$u_x = \partial_x u_x = u_y = u_z = \partial_x \theta = 0 \quad \text{on} \quad x = \pm\Gamma_x/2, \tag{4}$$

$$u_x = u_y = \partial_y u_y = u_z = \partial_y \theta = 0 \quad \text{on} \quad y = \pm\Gamma_y/2, \tag{5}$$

$$u_x = u_y = u_z = \partial_z u_z = \theta = 0 \quad \text{on} \quad z = \pm 1/2. \tag{6}$$

Following the procedures given in the preceding papers[10], the incompressible velocity field **u** is assumed to be represented in terms of the two roll variables ζ_1 and ζ_2

$$u_x = -\partial_y \zeta_2 - \partial_z \zeta_1, \quad u_y = \partial_x \zeta_2, \quad u_z = \partial_x \zeta_1 \tag{7}$$

where ζ_1 describes the horizontal parallel rolls extending periodically in the x direction, and ζ_2 is the vertical roll modes imposing the oscillatory type of perturbations on the basic horizontal rolls. Substitution of Eq.(7) in Eqs.(1)$\sim$(3) and elimination of $\delta p/\rho$ yield the equation of motion for the field variables ζ_1, ζ_2 and θ:

$$(\partial_t - \sigma\Delta)\partial_x^2 \Delta \zeta_1 - \sigma\partial_x(\partial_x^2 + \partial_y^2)\theta = \partial_x^2\partial_z F_x + \partial_x\partial_y\partial_z F_y - \partial_x(\partial_x^2 + \partial_y^2)F_z \tag{8}$$

$$(\partial_t - \sigma\Delta)\partial_x^2 \Delta \zeta_2 + \sigma\partial_x\partial_y\partial_z\theta = \partial_x^2\partial_y F_x - \partial_x(\partial_x^2 + \partial_z^2)F_y + \partial_x\partial_y\partial_z F_z \tag{9}$$

$$(\partial_t - \Delta)\theta - R\partial_x\zeta_1 = -F_\theta \tag{10}$$

where $F_i = u_j\partial_j u_i \quad (i = x, y, z)$ and $F_\theta = u_j\partial_j\theta$. The field variables are next expanded in terms of the basis functions which adequately represent the spatial structure of the convection rolls:

$$\zeta_1(x, y, z, t) = \sum_{\ell,m,n} C^{(1)}_{\ell,m,n}(t)\varphi_\ell(x/\Gamma_x)\chi_m(y/\Gamma_y)\Phi_{n(\ell,m)}(z) \tag{11}$$

$$\zeta_2(x,y,z,t) = \sum_{\ell,m,n} C^{(2)}_{\ell,m,n}(t)\varphi_\ell(x/\Gamma_x)\Psi_{m(\ell,n)}(y/\Gamma_y)\chi_n(z) \tag{12}$$

$$\theta(x,y,z,t) = \sum_{\ell,m,n} H_{\ell,m,n}(t)\psi_\ell(x/\Gamma_x)\psi_m(y/\Gamma_y)\chi_n(z) \tag{13}$$

where in accordance with Eqs.(4)$\sim$(6) the expansion functions satisfy the b.c. at $x = \pm 1/2$:

$$\varphi_\ell = \partial_x\varphi_\ell = \Phi_{\ell(m,n)} = \partial_x\Phi_{\ell(m,n)} = \Psi_{\ell(m,n)} = \partial_x\Psi_{\ell(m,n)} = \chi_\ell = \partial_x\psi_\ell = 0. \tag{14}$$

With the aid of the Galyorkin procedure, Eqs.(8)$\sim$(10) reduce to a system of the ordinary differential equations governing the mode amplitudes $\Xi(t) = \{\Xi_p(t); p = (\ell,m,n)\} = \{C^{(1)}_{\ell,m,n}(t), C^{(2)}_{\ell,m,n}(t), H_{\ell,m,n}(t)\}$ of the form

$$\partial_t\Xi = F(\Lambda,\Xi) \tag{15}$$

where the p-th component takes the form

$$\partial_t\Xi_p = F_p(\Lambda,\Xi) = \sum_{p'} L_{p,p'}\Xi_{p'} + \sum_{p'}\sum_{p''} N_{p;p',p''}\Xi_{p'}\Xi_{p''} \tag{16}$$

with Λ denoting the set of the control parameters $\Gamma_x, \Gamma_y, \sigma$ and R. The expressions for the coefficients $L_{p,p'}$, $N_{p;p',p''}$ are given elsewhere. The expansion functions appearing in Eqs.(11)$\sim$(13) are determined using the set of solutions to the following eigenvalue equations over the domain $-1/2 < x < 1/2$:

$$(\partial_x^4 - \alpha_\ell^4)\varphi_\ell = 0 \tag{17}$$

$$(\partial_x^2 + \beta_\ell^2)\psi_\ell = 0 \tag{18}$$

$$(\partial_x^2 + \gamma_\ell^2)\chi_\ell = 0 \tag{19}$$

$$(\partial_x^2 - (\alpha_m/\Gamma_x)^2 - (\gamma_n/\Gamma_y)^2)(\partial_x^2 + \lambda^2_{\ell(m,n)} - (\alpha_m/\Gamma_x)^2 - (\gamma_n/\Gamma_y)^2)\Phi_{\ell(m,n)} = 0 \tag{20}$$

$$((\partial_x/\Gamma_y)^2 - (\alpha_m/\Gamma_x)^2 - \gamma_n^2)((\partial_x/\Gamma_y)^2 + \mu^2_{\ell(m,n)} - (\alpha_m/\Gamma_x)^2 - \gamma_n^2)\Psi_{\ell(m,n)} = 0 \tag{21}$$

where the b.c. are defined by Eq.(14) while the eigenvalues are denoted by α_ℓ, β_ℓ, γ_ℓ, $\lambda_{\ell(m,n)}$, and $\mu_{\ell(m,n)}$. Equation (16) contains an infinite number of mode variables. In the following, however, Eq.(16) is further reduced to a truncated form which includes only a finite number of mode variables most relevant to the preblem.

§3. Computational results

We consider in this paper the system characterized by the external parameters $\sigma = 7$, $\Gamma_x = 10$ and $\Gamma_y = 4$. For this case, it was experimentally shown that onset of thermal convection occurs typically in the form of 10 parallel rolls whose axes are in the y direction, and that the 10-roll convection state becomes at $R = 8.6R_c$ structurally unstable and turns into the 6-roll state.[6] For describing this behavior of convection, we construct a model system consisting of the mode variables for the 10- and the 6-roll states. This means that the model includes 2 velocity and 3 temperature modes in the x direction. The number of the modes in the other directions are chosen conveniently: 8 and 2 modes in the y and z directions recpectively. To be more specific, the mode variables thus retained are given by

$$X = \{C^{(1)}_{\ell o,me,1q}, C^{(1)}_{\ell o,mo,1q}, C^{(2)}_{\ell o,me,1q}, C^{(2)}_{\ell o,mo,1q}, H_{(k+1)e,me,1q}, H_{(k+1)e,mo,1q} \\ |\ell = 3,5; m = 1,2,3,4; q = e,o; k = 0,3,5\} \tag{22}$$

where e and o mean even and odd respectively, and the thermal modes specified by $k = 0$ are spatially uniform in the x direction. This truncation contains 112 variables in all. Substitution of Eq.(22) in Eq.(16) gives the truncated form

$$\partial_t X = F(X) = L(X) + N(X,X), \tag{23}$$

or more precisely,

$$\partial_t X_p = \sum_{p'} L_{p,p'} X_{p'} + \sum_{p'} \sum_{p''} N_{p;p',p''} X_{p'} X_{p''} \tag{24}$$

for $p = 1,2,\ldots,N(=112)$. The steady state X^0 of Eq.(23) is determined by a solution of

$$F(X) = 0 \tag{25}$$

and its stability is governed by the associated variational equation

$$\partial_t \delta X = DF(X^0)\delta X \tag{26}$$

where $DF(X^0)$ is the Jacobian matrix of the vector field $F(X)$ evaluated at X^0. For convenience, we use the reduced Rayleigh number $r = R/R_{c0}$ ($R_{c0} = 1710$) for specifying the imposed temperature gradient. The steady state solutions given below were obtained as follows: First, a steady solution is obtained by direct numerical time integration of Eq.(23). Once X^0 is found for some value of r, its slightly varied form for a neighboring value of r can be easily obtained using the Newton method. It should be noted here, however, that the convergence rate of its successive approximations turns out very slow when the relevant steady state becomes unstable. This in turn gives us information on the instability point of the system.

For our model consisting of the 10- and 6-roll modes, the transition from thermal conduction to convection occurs at $R_c = 2190 = 1.28R_{c0}$. This is determined as the point where the largest eigenvalue of $DF(X = 0)$ changes its sign from negative to positive. Actually, there are two eigenmodes which become unstable almost simultaneously with increase of R. As is given in Figs.1 by the isopleths of the associated eigenvectors, these instabilities trigger the emergence of the 10- and the 6-roll states. The results thus account for the experimental situations in which some kind of flow induction is necessary to prepare a convection state with a well-defined number of the rolls. Figure 2 show the isopleths for the 10-roll convection state prevailing at $r = 1.55$. The motion is found to be predominantly two-dimensional. This 10-roll state dominates the system over a range of R above R_c. When R is increased to $r_{c1} = 6.66$, however, the system undergoes a structural transition to the 6-roll state with cross-roll deformations. This can be seen from the isopleths in Fig.3 for the unstable eigenmode initiating this transition and the isopleths in Fig.4 for the velocity field for the resulting

convection state at $r = 6.71$ slightly above r_{c1}. The unstable mode is charaterized by the wavenumbers $\alpha_x = 1.88$ and $\alpha_y = 2.36$. This transition is considered to corespond to the above-mentioned experimentally observed one occurring at $r = 8.6$. Although the prevailing state is now dominated by the 6-roll state, it still contains some trace of the 10-roll mode amplitudes. In this sense, the result differs from the experimental one in which the convection state above r_{c1} consists entirely of the 6-roll state with weak cross-roll perturbations.

This state stably persists up to $r = 13.1$ where it undergoes the transition to the state shown in Fig.5. The 6-roll state now entirely dominates the convection and the wavelength of the cross-roll perturbations becomes shorter. With further increase of r, the Hopf bifurcation occurs at $r = 14.9$ and the convection develops slow time oscillations with the frequency of the order of 10 mHz. In fact, the PSD in Fig.6 shows that the frequency at $r = 14.9$ is given by $g_1 = 9.6$ mHz. By contrast, the experimental observation gives the results that the 6-roll steady state becomes time-dependent at $r = 13.4$ and its frequency is $f_1 = 0.9$ mHz.[6] Hence, our coupled-mode system consisting of the 10- and the 6-roll variables gives rise to the periodic oscillations whose frequency g_1 is by a factor of 10 larger than that f_1 obtained from the experiment. Incidentally, the oscillating convection arising from the oscillatory instability in a small-aspect-ratio vessel is usually associated with the frequency of the order of 100 mHz. When R is increased still further, the prevailing oscillatory motion loses its periodicity and turns into chaotic. This can be seen from the PSD at $r = 16.4$ shown in Fig.6(b) where line spectral components completely disappear. However, we have not clarified what mechanism entails the transition from the periodic to the chaotic motion. In experiments, in addition to the slow oscillations given above, the convection with further increase of r gives rise to the rapid oscillating modes which are characterized by the frequencies of the order of 100 mHz and occur over some localized

regions of the convection cell.[8),9)] Our present 10- and 6-roll model cannot describe this kind of localized rapid oscillations.

Since the convection is found to be dominated by the 6-roll state at higher values of r, it is worth while to study its spatio-temporal behavior using a model slightly different from that given above. First, we consider a system consisting of the mode variables for the 6- and the 8-roll states. The retained mode variables are the same as those given in Eq.(22) except that the mode suffices denoted by ℓ=5 and k=5 in Eq.(22) are now replaced by those ℓ=4 and k=4 respectively. In the model thus obtained, the 6-roll state predominates over the convection patterns even for lower values of r. In this sense, it cannot describe the structural transition from the 8-roll to the 6-roll state such as observed in experiments. Further increase of r to r=14.7 touches off a real mode instability and the steady state persistent thus far becomes unstable. As a result, the convection develops extremely slow oscillations whose frequency is at r=15.1 given by g_2=2.2 mHz, which is shown by the PSD in Fig.7. The frequency g_2 appearing here is of the same order as that f_1 observed in experiments.[6)] This shows the possibility that the extremely low frequency oscillations peculiar to intermediate-aspect-ratio experiments are involved by the nonlinear couplings between the modes whose roll wavelengths are slightly different from one another.

We next consider a model consisting of the 6- and the 12-roll mode states. This is obtained by replacing in Eq.(22) the mode suffices ℓ=5 and k=5 by those ℓ=6 and k=6. Here, the fundamental 6-roll modes couples with the secondary higher harmonic modes specified by the 12-roll modes. A combination of this type of the mode variables is very common to nonlinear dynamical models. The predominantly 6-roll state undergoes at r=9.8 the Hopf bifurcation leading to periodic oscillations. The PSD in Fig.8(a) shows that the motion at r=10.5 is singly periodic and oscillates with the frequency g_3=117 mHz. With further increase of r, the motion becomes quasi-periodic. This is shown

in Fig.8(b) in that the motion at r=12.3 contains the two fundamental frequencies: g_3=113 mHz and g_4=15 mHz. In the experiments, in addition to the extremely slow oscillations f_1, the convection with increase of r comes to develop fast periodic oscillations whose frequencies take such values as f_2=145 mHz and f_3=160 mHz at r=17.6.[6] If the oscillatory modes denoted by f_2 and f_3 in the experiments correspond to those denoted by g_3 and $g_3 + g_4$ in our results, the origin of the fast oscillatory motion appearing at higher values of r is considered to be attributable to the nonlinear couplings between the fundamental 6-roll modes and its secondary higher harmonic modes.

References

1) J.P. Gollub and S.V. Benson, J. Fluid Mech. **100**(1980), 449.

2) A. Libchaber, S. Fauve and C. Laroche, Physica **7D**(1983), 73.

3) J.P. Gollub, A.R. McCarriar and J.F. Steinman, J. Fluid Mech. **125**(1982), 259.

4) P. Kolodner, R.W. Walden, A. Passner and C.M. Surko, J. Fluid Mech. **163**(1986), 195.

5) R.W. Motsay, K.E. Anderson and R.P. Behringer, preprint.

6) S. Nasuno, M. Sano and Y. Sawada, preprint.

7) F.H. Busse and R.M. Clever, J. Fluid Mech. **91**(1979), 319.

8) R.W. Walden, P. Kolodner, A. Passner and C.M. Surko, Phys. Rev. Lett. **53**(1984), 242.

9) S. Sato, M. Sano and Y. Sawada, preprint.

10) H. Yahata, Progr. Theor. Phys. **75**(1986), 790; **78**(1987), 282.

Figure Captions

Fig.1 The isopleth of the velocity field $u_x(x, y, z = 1/4)$ for the eigenmode initiating the onset of thermal convection. (a) the 6-roll state; (b) the 10-roll state.

Fig.2 The isopleth of the velocity field $u_x(x, y, z = 1/4)$ at r=1.55.

Fig.3 The isopleth of the velocity field $u_x(x, y, z = 1/4)$ for the eigenmode initiating the structural transition at r=6.66.

Fig.4 The isopleth of the velocity field $u_x(x, y, z = 1/4)$ for the resultant convection state at r=6.71.

Fig.5 The isopleth of the velocity field $u_x(x, y, z = 1/4)$ at r=13.1 for the convection state arising as a result of the secondary structural transition.

Fig.6 The PSD for the mode amplitude $C^{(1)}_{5o,1o,1e}(t)$ at (a) r=14.9 and (b) r=16.4. The abscissa measures the frequency in unit of 19.74 κ/d^2=115 mHz for d=0.5 cm and $\kappa = 1.454 \times 10^{-3}$ cm^2/s.

Fig.7 The PSD for the mode amplitude $C^{(1)}_{4o,1o,1e}(t)$ at r=15.1. The abscissa measures the frequency in unit of $16.19\kappa/d^2$ =94.2 mHz.

Fig.8 The PSD for the mode amplitude $C^{(1)}_{3o,1e,1e}(t)$ at (a) r=10.5 and (b) r=12.3. The abscissa measures the frequency in unit of $13.42\kappa/d^2$=78.1 mHz.

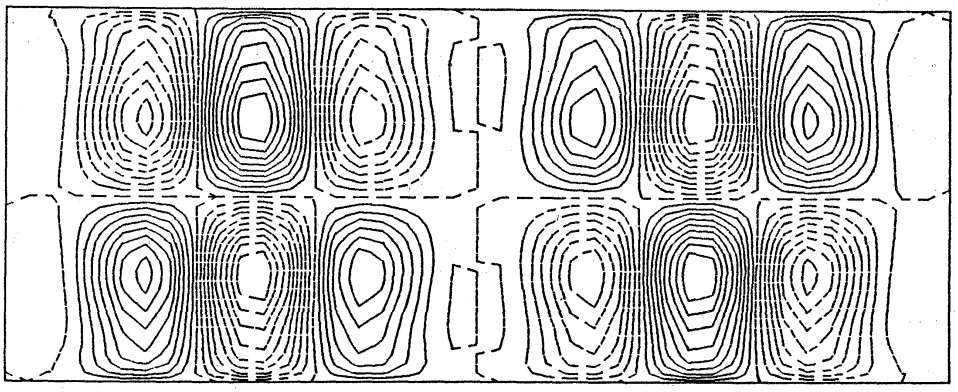

Fig.1(a)

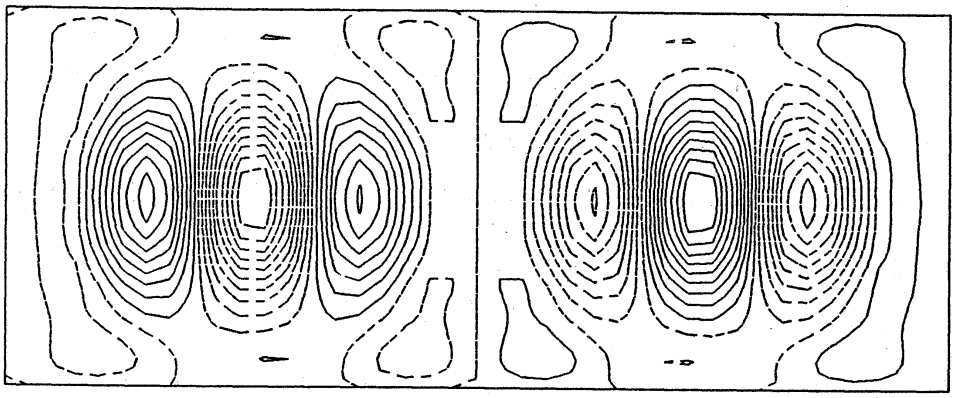

Fig.1(b)

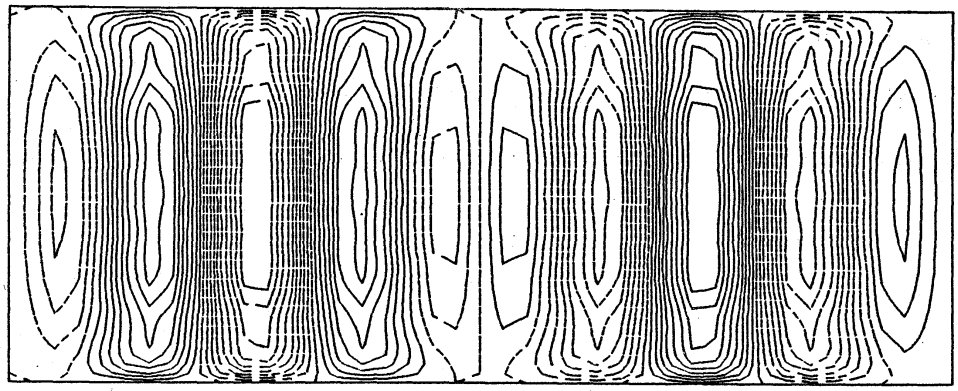

Fig.2

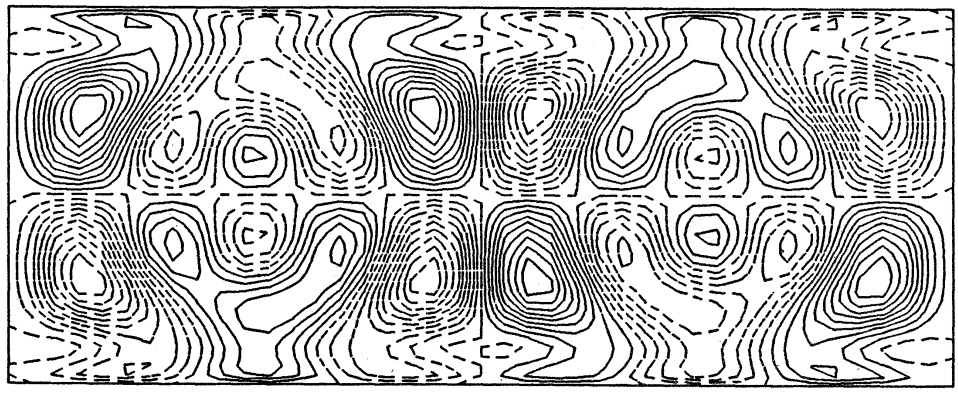

Fig.3

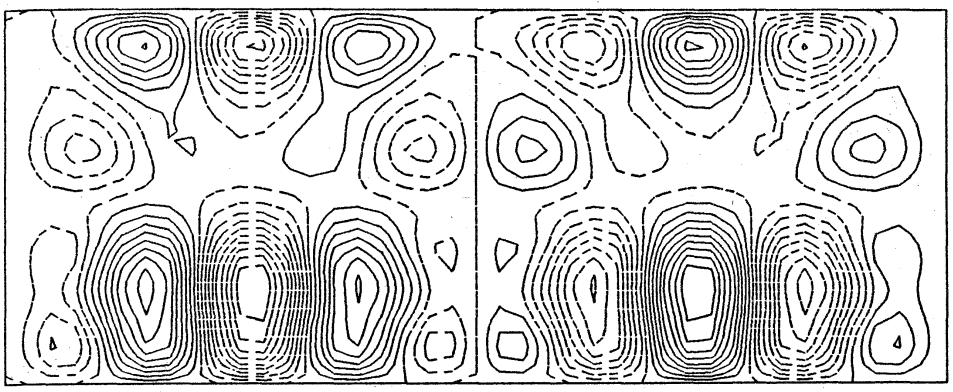

Fig.4

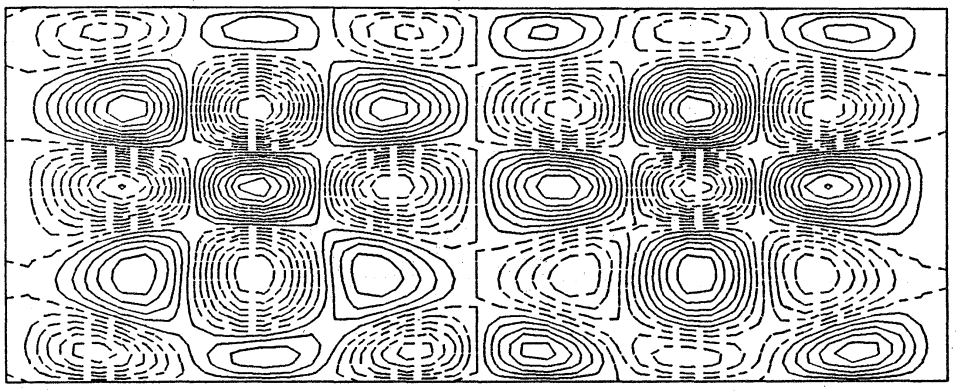

Fig.5

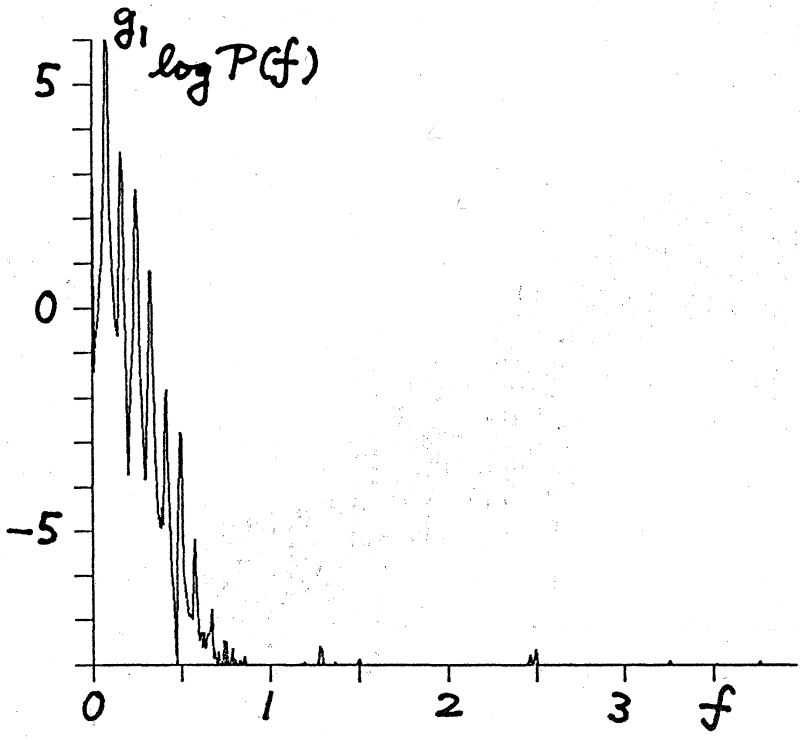

Fig.6(a)

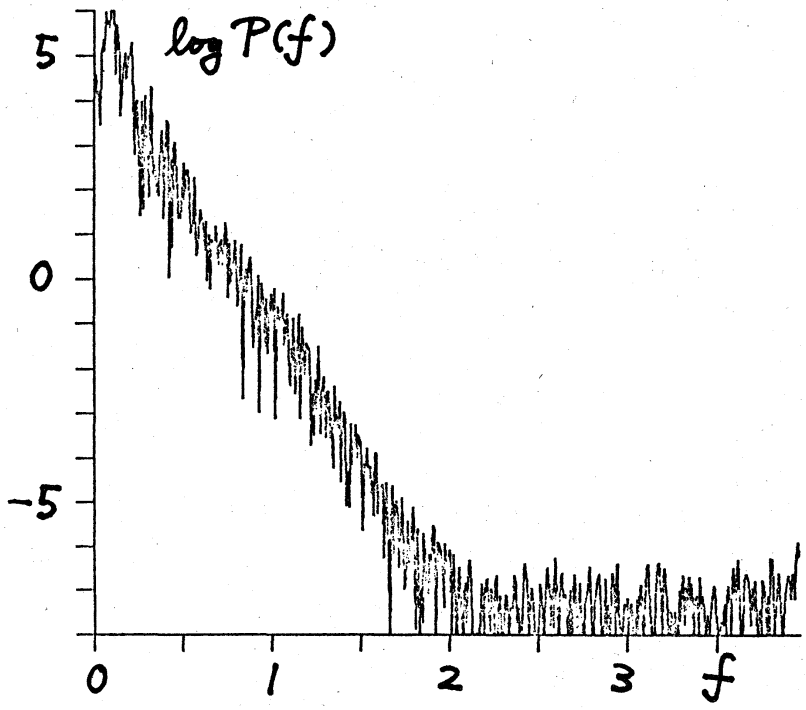

Fig. 6(b)

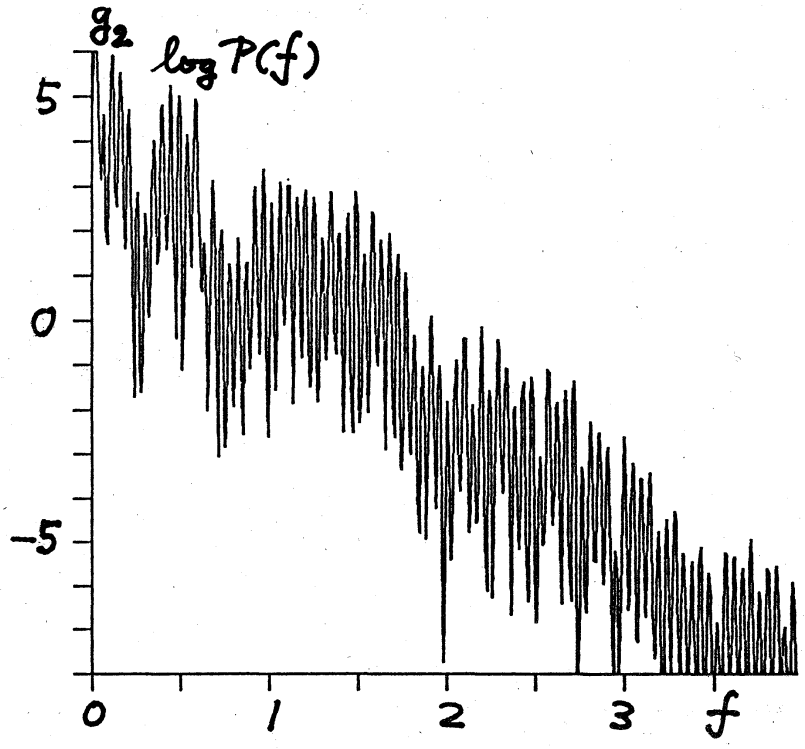

Fig. 7

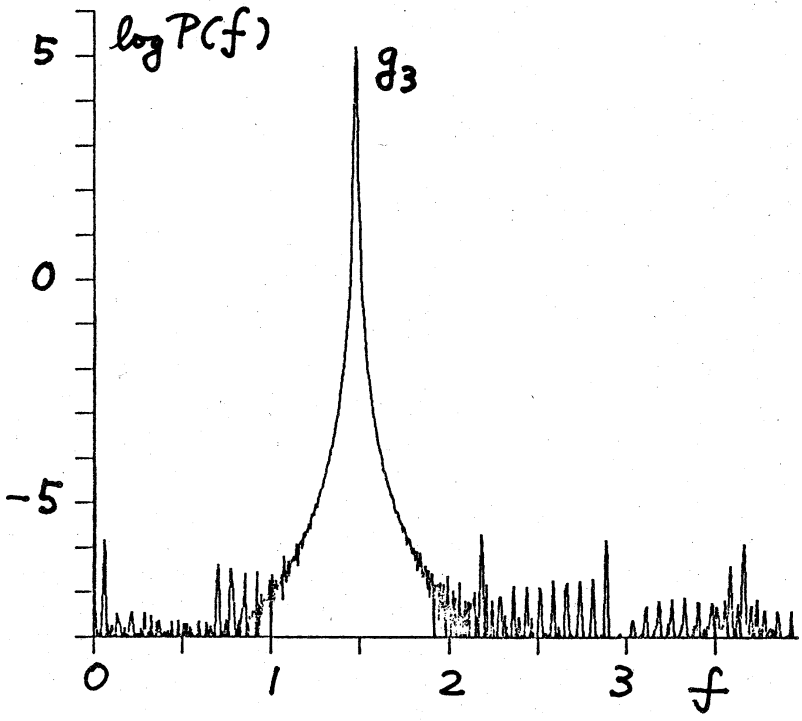

Fig. 8(a)

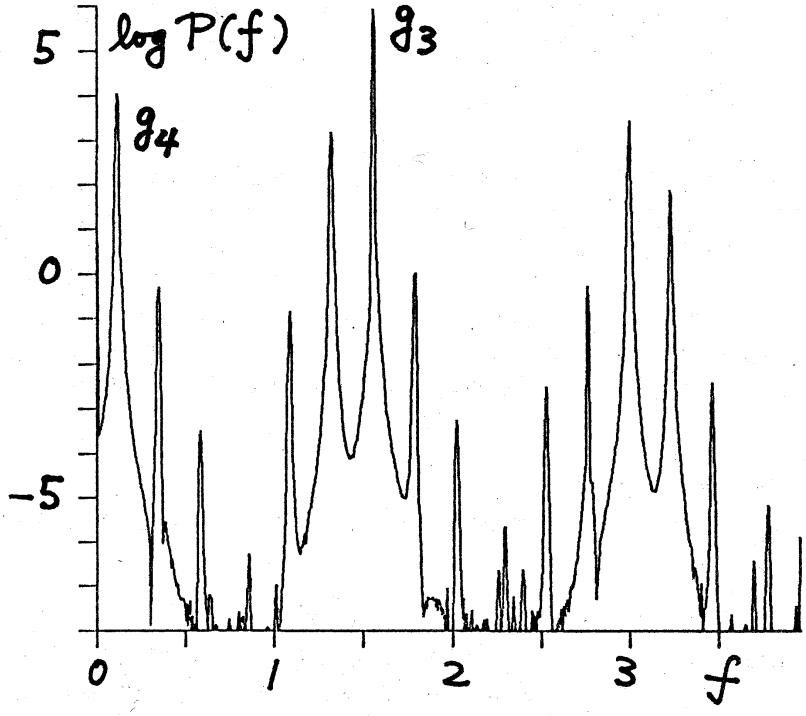

Fig. 8(b)